Research Article

PHOTONICS Research

Passive parity-time-symmetry-breaking transitions without exceptional points in dissipative photonic systems [Invited]

YOGESH N. JOGLEKAR* AND ANDREW K. HARTER

Department of Physics, Indiana University-Purdue University Indianapolis (IUPUI), Indianapolis, Indiana 46202, USA
**Corresponding author: yojoglek@iupui.edu*

Received 11 January 2018; revised 14 June 2018; accepted 28 June 2018; posted 2 July 2018 (Doc. ID 314689); published 24 July 2018

Over the past decade, parity-time (PT)-symmetric Hamiltonians have been experimentally realized in classical, optical settings with balanced gain and loss, or in quantum systems with localized loss. In both realizations, the PT-symmetry-breaking transition occurs at the exceptional point of the non-Hermitian Hamiltonian, where its eigenvalues and the corresponding eigenvectors both coincide. Here, we show that in lossy systems, the PT transition is a phenomenon that broadly occurs without an attendant exceptional point, and is driven by the potential asymmetry between the neutral and the lossy regions. With experimentally realizable quantum models in mind, we investigate dimer and trimer waveguide configurations with one lossy waveguide. We validate the tight-binding model results by using the beam-propagation-method analysis. Our results pave a robust way toward studying the interplay between passive PT transitions and quantum effects in dissipative photonic configurations.

OCIS codes: (080.1238) Array waveguide devices; (270.5585) Quantum information and processing.

https://doi.org/10.1364/PRJ.6.000A51

1. INTRODUCTION

A fundamental principle of traditional quantum theory is that the observables of a system are Hermitian operators [1]. This self-adjoint character of observables is defined with respect to a global (Hamiltonian-independent) Dirac inner product. In particular, the Hamiltonian of a closed quantum system is Hermitian. It determines the energy levels of the system and therefore the experimentally observable transition frequencies. Thus, it came as a great surprise when Carl Bender and co-workers discovered a broad class of non-Hermitian, continuum Hamiltonians with purely real spectra [2,3]. The salient feature of such Hamiltonians is the presence of complex potentials $V(x)$ that are invariant under the combined parity ($P: x \to -x$) and time-reversal ($T = *$) operations, i.e., $V^*(-x) = V(x)$. Initial efforts on this subject focused on developing a self-consistent complex extension of quantum mechanics via a redefinition of the inner product that is used to define the adjoint of an observable [4,5]. This line of inquiry led to significant mathematical developments in understanding the properties of pseudo-Hermitian operators [6–11]. But it did not elucidate a simple physical picture for complex potentials that are a hallmark of parity-time (PT)-symmetric Hamiltonians.

Experimental progress on the PT-symmetric systems started with two realizations [12,13]. First, the Schrödinger equation is isomorphic, with paraxial approximation to the Maxwell's equation, where the local index of refraction $n(x) = n_R(x) + in_I(x)$ plays the role of the potential $V(x)$. Second, it is easy to engineer a lossy index of refraction $n_I(x) < 0$ and not too difficult to engineer a gain either, i.e., $n_I(x) > 0$. These dual realizations provided a transparent, physical insight into the meaning of complex, PT-symmetric potentials: they represent balanced, spatially separated loss and gain [14]. Since then, over the past decade, coupled photonic systems described by non-Hermitian, PT-symmetric effective Hamiltonians have been extensively investigated [15–22]. Light propagation in such systems shows nontrivial functionalities, such as unidirectional invisibility [23,24], that are absent in their no-gain, no-loss counterparts. We emphasize that these realizations are essentially classical. Gain at the few-photons level is random due to spontaneous emission [25,26]; in contrast, loss is linear down to the single-photon level. Thus, engineering a truly quantum PT-symmetric system is fundamentally difficult. Therefore, in spite of a few theoretical proposals [27], there are no experimental realizations of such systems that show quantum correlations present.

By recognizing that a two-state loss-gain Hamiltonian is the same as a two-state loss-neutral Hamiltonian apart from an "identity-shift" along the imaginary axis, the language of

PT-symmetry and PT transitions has been adopted to purely dissipative, classical systems as well [28]. Indeed, the first ever observation of PT-symmetry breaking was in two coupled waveguides, one with loss γ and the other without [29]. As the loss strength was increased from zero, the net transmission first decreased from unity, reached a minimum, and then increased as γ was increased beyond a threshold, signaling the passive PT-symmetry-breaking transition. This mapping provided a clear way forward to define the passive PT-symmetry-breaking phenomenon in truly quantum, effectively two-level, dissipative systems. It led to the first observations of PT-symmetry breaking in the quantum domain with quantum-correlated single photons [30] and ultracold atoms [31].

In this paper, we extend the notion of passive PT transition to lossy Hamiltonians that do not map onto a PT-symmetric Hamiltonian. By using tight-binding models and beam-propagation-method (BPM) analysis of experimentally realistic setups, we demonstrate that such transitions–driven by the emergence of a slowly decaying eigenmode–occur without the presence of exceptional points.

2. AVOIDED LEVEL CROSSING IN GAIN-LOSS SYSTEMS

The prototypical effective Hamiltonian for experimentally realized, classical gain-loss systems is given by $H_{\rm PT}(\gamma) = -J\sigma_x + i\gamma\sigma_z \neq H_{\rm PT}^{\dagger}$, where σ_k are the standard Pauli matrices. This Hamiltonian is invariant under combined operations of $P = \sigma_x$ and $T = *$. With $\hbar = 1$, the parameters of the Hamiltonian $H_{\rm PT}$ have units of $\rm s^{-1}$. In optical settings, the time is proportional to the distance z traveled along the waveguide; therefore, the intersite coupling J is inversely proportional to the coupling length L_c, i.e., $J = \pi c/(n_0 L_c)$, where c/n_0 is the constant speed of light in the waveguide with local index n_0. Similarly, the loss γ and the potential offset δ (measured in $\rm s^{-1}$) are linearly proportional to the inverse penetration depth and the propagation-constant offset (measured in $\rm m^{-1}$), respectively. The eigenvalues of $H_{\rm PT}$ are given by $\pm\sqrt{J^2 - \gamma^2}$, are real for $\gamma \leq J$, and become a complex conjugate pair for $\gamma > J$. The transition from the PT-symmetric phase, i.e., purely real eigenvalues, to PT-symmetry-broken phase, i.e., some complex-conjugate eigenvalues, occurs at the threshold $\gamma_{\rm PT} = J$. At this point, eigenvalues and eigenvectors of $H_{\rm PT}(\gamma)$ both become degenerate. Thus the PT-symmetry-breaking transition point is the same as the second-order exceptional point of the Hamiltonian $H_{\rm PT}$ [32].

What happens when this Hamiltonian is perturbed by an antisymmetric real potential? Without loss of generality, such potentials can be implemented by $i\gamma \to i\gamma + \delta$. The eigenvalues of the perturbed Hamiltonian $H(\gamma, \delta)$ immediately become complex:

$$\lambda_{\pm}(\gamma, \delta) = \pm\sqrt{J^2 - \gamma^2 + \delta^2 - 2i\gamma\delta}. \quad (1)$$

Figure 1 shows that when $\delta > 0$, for $\gamma \ll J$, the imaginary parts $\Im\lambda_{\pm}$ are quite small and grow linearly with γ. This behavior changes to a steep $d\Im\lambda_{\pm}/d\gamma$ at $\gamma = J$, signaling the enhanced sensitivity in the neighborhood of the exceptional point [33,34]. However, the eigenvalues are always complex, and therefore, the system is never in the PT-symmetric phase when $\delta \neq 0$. Thus, the notion of a PT-symmetry-breaking transition cannot be extended to perturbed gain-loss Hamiltonians $H(\gamma, \delta)$.

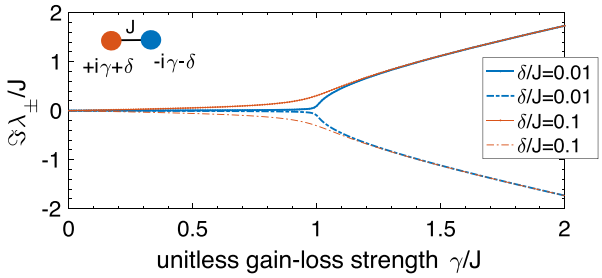

Fig. 1. Imaginary parts of the spectrum Eq. (1) for nonzero perturbations $\delta/J = \{0.01, 0.1\}$. The schematic PT dimer with gain (red) and loss (blue) sites is shown. When $\gamma/J \ll 1$, $\Im\lambda_{\pm}$ grow linearly with the gain-loss strength, but are nonzero. The divergence of their derivative at the threshold $\gamma = J$ is smoothed out as $\delta > 0$ increases. In this case, the system is always in the PT-broken phase, no matter how small $\Im\lambda_{\pm}(\gamma) \neq 0$ are.

In true gain-loss systems, the PT-symmetry breaking, defined by real-to-complex spectrum, occurs at the exceptional point, defined by coincidence of both eigenvalues and eigenvectors. Note that similar avoided level crossings [35–37] also occur in coupled lasers with static cavity losses and pump-current controlled gains and show surprising phenomena, such as pump-induced laser death [38,19], loss-induced revival of lasing [20], and laser self-termination [39,40].

3. PT-SYMMETRY BREAKING IN DISSIPATIVE SYSTEMS

The prototypical Hamiltonian for experimentally realized neutral-loss systems is given by

$$H_D(\gamma) = -J\sigma_x - i\gamma(1 - \sigma_z) = -J\sigma_x - 2i\gamma|2\rangle\langle 2|. \quad (2)$$

In the quantum context, this represents a two-state system with loss only in the second state. In the classical context, this represents two evanescently coupled waveguides, where there is absorption only in the second waveguide [29]. Note that $H_D(\gamma) = H_{\rm PT}(\gamma) - i\gamma 1_2$; however, due to the imaginary shift that is not invariant under time-reversal operation, the dissipative Hamiltonian does not commute with the antilinear PT operator, i.e., $[{\rm PT}, H_D] \neq 0$. The eigenvalues of Eq. (2) are given by $\lambda_{D\pm} = -i\gamma \pm \sqrt{J^2 - \gamma^2}$ and always have positive decay rates $\Gamma_{\pm} = -\Im\lambda_{D\pm}$ for the two eigenmodes of the lossy Hamiltonian H_D. When $\gamma \leq J$, the two decay rates are equal, and they increase linearly with γ, i.e., $d\Gamma_{\pm}/d\gamma > 0$. Traditionally, this region is called the PT-symmetric phase. When $\gamma = J$, the corresponding eigenmodes become degenerate. However, when $\gamma > J$, the decay rate for one of the eigenmodes starts to become smaller:

$$\Gamma_{+} = \gamma - \sqrt{\gamma^2 - J^2} \underset{\gamma \gg J}{\to} \frac{J^2}{2\gamma}, \quad (3)$$

while the second mode decays faster with $\Gamma_{-} \to 2\gamma$. Traditionally, this region is called the PT-broken phase. We define the emergence of a slowly decaying mode, i.e.,

$$\frac{d\Gamma}{d\gamma} = 0 \text{ at } \gamma = \gamma_{PT}, \tag{4}$$

as the defining characteristic of the passive PT transition in loss-neutral systems [29–31]. Indeed, the increased total transmission with increasing loss seen in Ref. [29] is due to this mode. We note that this criterion, defined by the sign of $d\Gamma/d\gamma$ changing from positive to negative for one of the modes, is not equivalent to defining the transition by the presence of an exceptional point, where the two decaying eigenmodes coalesce. For the identity-shifted Hamiltonian $H_D(\gamma)$, Eq. (2), they happen to coincide. The latter criterion is only meaningful for the identity-shifted cases, whereas Eq. (4) is physically motivated and has straightforward experimental consequences [29–31].

In the following sections, we elucidate the consequences of this difference between dissipative PT systems and gain-loss systems for dimer and trimer models, while keeping evanescently coupled photonic waveguides in mind as their experimental realizations.

4. DISSIPATIVE PT DIMER AND TRIMER CASES

Starting from the dissipative dimer Hamiltonian H_D, Eq. (2), we now consider its Hermitian, onsite perturbation:

$$H_2(\gamma,\delta) = \begin{pmatrix} 0 & -J \\ -J & -2i\gamma - 2\delta \end{pmatrix}. \tag{5}$$

Note that $H_2(\gamma,\delta)$ represents two waveguides with evanescent coupling J, with a loss potential 2γ in the second waveguide and an extra onsite potential -2δ, which is generated by an offset in the real part of the index of refraction vis-à-vis the first waveguide.

It is straightforward to analytically obtain the eigenvalues $\lambda_{2D\pm}$ of $H_2(\gamma,\delta)$, similar to those in Eq. (1), and the corresponding eigenvectors. Analyzing their behavior in the neighborhood of $\gamma/J = 1, \delta = 0$ requires further care, as it entails developing the corresponding Puiseux series in fractional powers of the distance from the exceptional point [32–34]. In this paper, we primarily focus on numerical results across the entire parameter space instead of analytical results in the vicinity of the exceptional point. Figure 2 shows the evolution of the decay rates $\Gamma_\pm(\gamma)$ for the two eigenmodes as a function of the onsite perturbation. When $\delta = 0$, the exceptional point and the passive PT-symmetry-breaking threshold, defined by the emergence of the slowly decaying mode, coincide. When $\delta/J = 0.1$, the decay rates for the two modes are always different. Initially, both increase with γ until near $\gamma \sim J$, where one takes off and the other starts to decrease, thus indicating the emergence of the slowly decaying mode. When the perturbation is increased further, $\delta/J = 0.8$, a similar behavior is observed, but on a weaker scale. The inset in Fig. 2 shows the numerically obtained derivative of the decay rate of the slow mode, $d\Gamma_+/d\gamma$. When $\delta = 0$, we see that it is unity for $\gamma < J$ and diverges to $-\infty$ as $\gamma \to J^+$. For $\delta > 0$, the inset provides a quick determination of the PT transition threshold γ_{PT}. These results are even in δ, and the emergence of a slowly decaying mode is a robust feature for all offsets $\delta \neq 0$. We would like to point out that in the dissipative case, the avoided-level-crossing location is instrumental to determining the passive PT transition point. In contrast, the counterintuitive phenomena in coupled lasers do not occur at the avoided-level-crossing location, but at the location where an amplifying mode emerges [39,40].

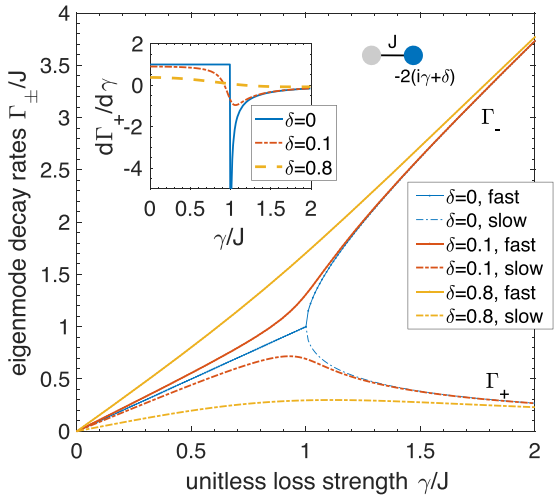

Fig. 2. Decay rates $\Gamma_\pm$ of the two eigenmodes of Eq. (5) show the emergence of a slowly decaying mode for $\gamma \sim J$, not only at $\delta = 0$, the prototypical exceptional point case, but also for a wide range of $\delta/J \neq 0$. Inset: the PT transition threshold is determined by $d\Gamma/d\gamma$ changing its sign from positive to negative. These results are even in the offset δ and thus remain the same for $\delta < 0$.

There is no exceptional point for the Hamiltonian $H_2(\gamma, \delta \neq 0)$, and yet the passive PT transition phenomenon, defined by the emergence of a slow mode, is robust for $\delta \neq 0$. To show this, we obtain a key experimental signature [29], the total transmission $T(\gamma,\delta)$ as a function of the onsite potential δ. Starting from an initial injection into the first, neutral site, i.e., $|\psi(0)\rangle = |1\rangle$, the total transmission at time t (or equivalently at distance $z = ct/n_0$ traveled along the waveguide) is given by $T \equiv \langle\psi(t)|\psi(t)\rangle$, where $|\psi(t)\rangle = \exp(-iH_2 t)|\psi(0)\rangle$. Keeping in mind Ref. [29], we obtain the net transmission at a single-coupling length, i.e., $z = L_c$, or equivalently, $t = \pi/J$. Figure 3 shows that $T(\gamma,\delta)$ has a robust upturn feature for all δ, from $\delta = 0$ to a large value of $\delta/J \sim 1$; it means that the key signature used in the passive PT-symmetry-breaking experiments [29] does not probe the exceptional point, but rather, the slowly decaying mode. The results in Fig. 3 bolster the rationale for using Eq. (4) as the definition of passive PT-symmetry-breaking transition with or without exceptional points.

Let us now consider a dissipative trimer with only one lossy waveguide. The nearest-neighbor tunneling Hamiltonian for a trimer with open boundary conditions is given by $H_0 = -J(|1\rangle\langle 2| + |2\rangle\langle 3| + \text{h.c.})$. With loss and a different onsite potential in the central waveguide, the trimer Hamiltonian becomes

$$H_{tc} = H_0 - (i\gamma + \delta)|2\rangle\langle 2|. \tag{6}$$

Equation (6) has one zero eigenvalue with an antisymmetric eigenmode that does not couple to the central, lossy site.

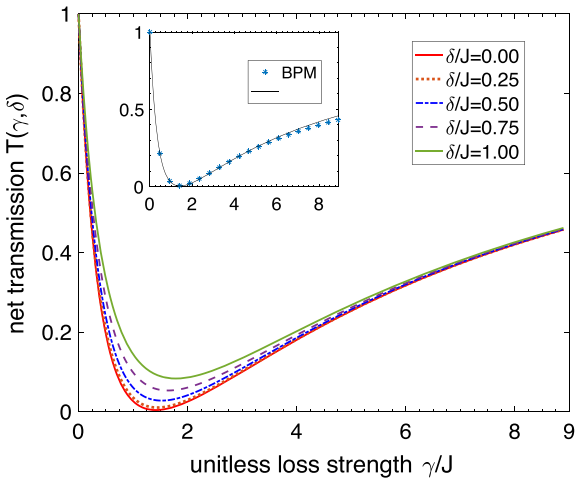

Fig. 3. Net transmission $T(\gamma)$ shows an upturn with increasing loss strength γ signaling the passive PT transition [29]. It shows minimal change from its $\delta = 0$ value [29] when δ/J is increased all the way to unity, i.e., the system is removed far from the exceptional point. These results are even in δ and thus remain unchanged for $\delta < 0$. Inset: the lattice-model results (line) are consistent with the BPM results (stars) obtained with sample parameters in Ref. [29]; see Section 5 for details.

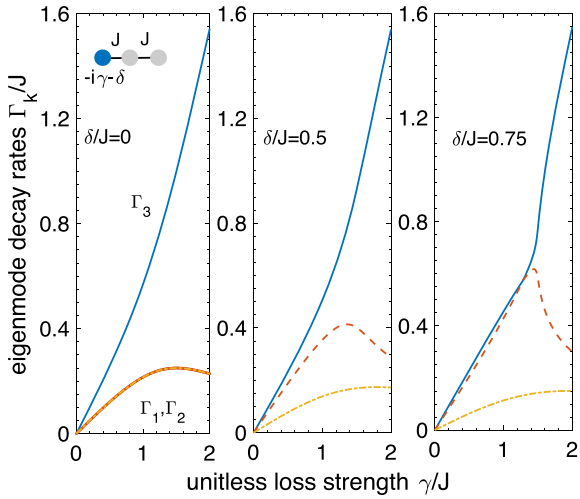

Fig. 5. PT transition in three coupled waveguides with first lossy waveguide, Eq. (7). When $\delta = 0$, the two modes with equal decay rates undergo a sign change for $d\Gamma_k/d\gamma$ near $\gamma/J \sim 1.4$. When onsite potential $\delta > 0$ is introduced, the two degenerate modes split, and the eigenmode decay-rate diagram hints at the existence of an exceptional point at $\delta/J = 0.75$.

The other two eigenvalues are given by $[-(i\gamma + \delta) \pm \sqrt{8 - (\gamma - i\delta)^2}]/2$. Figure 4 shows the decay rates for the three modes as a function of the loss γ and onsite potential δ in the central waveguide. The zero decay rate, $\Gamma_1 = 0$, denotes the antisymmetric eigenmode. When $\delta = 0$, we see that the Hamiltonian H_{tc} has an exceptional point at $\gamma_{PT} = 2\sqrt{2}J$. For $\gamma < \gamma_{PT}$, both decay rates Γ_2, Γ_3 increase with loss strength, and the system is in the PT-symmetric phase. It is characterized by a net transmission that decreases when γ is increased. When $\gamma > \gamma_{PT}$, the decay rate Γ_2 starts to decrease and, as a result, the total transmission is increased with increasing γ [29–31]. When $\delta \neq 0$, these features remain robust, but the Hamiltonian H_{tc} does not have an exceptional point.

If the loss is in one of the outer waveguides, the trimer Hamiltonian is given by

$$H_{te} = H_0 - (i\gamma + \delta)|1\rangle\langle 1|. \tag{7}$$

Figure 5 shows the eigenmode decay rates Γ_k as a function of the loss strength γ for various onsite potentials δ. When $\delta = 0$, the trimer has two modes with equal decay rates, $\Gamma_1 = \Gamma_2$, and a third one with the fastest decay rate, Γ_3. Near $\gamma/J \sim 1.4$, the former two change over to slowly decaying modes, signifying the PT transition. As $\delta > 0$ is increased, the two degenerate decay rates split, and faster of the two, Γ_2, approaches the third one, Γ_3. Results in the last panel, corresponding to $\delta/J = 0.75$, hint at the existence of an exceptional point in the vicinity of these parameters. In general, similar results are found for multiple losses and/or onsite potentials for the trimer model. The emergence of slowly decaying modes is commonplace, even when the existence of exceptional points is not.

Lastly, we consider a trimer with periodic boundary conditions, with the Hamiltonian

$$H_t(\gamma, \delta, J') = H_{tc} - J'(|1\rangle\langle 3| + |3\rangle\langle 1|), \tag{8}$$

where $0 \leq J' \leq J$ denotes the tunable coupling between the first and the third waveguides. This ring configuration can be easily realized via femtosecond-laser direct-written waveguides in glass [41]. We leave as an exercise for the reader to verify the following results. The antisymmetric mode continues to be an eigenmode of the Hamiltonian H_t with real eigenvalue $+J'$. The other two decaying eigenmodes have eigenvalues given by

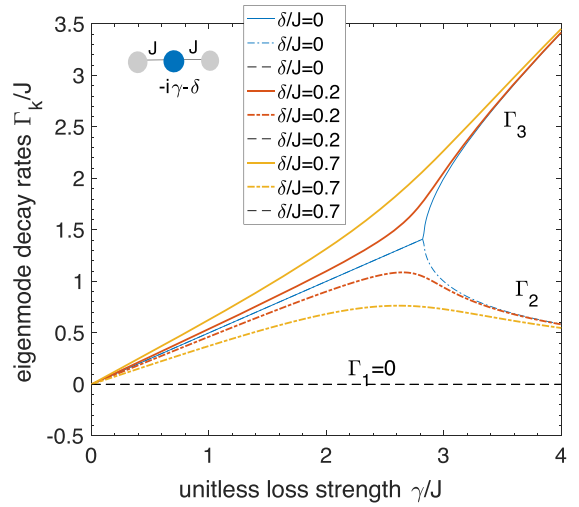

Fig. 4. PT transition in three coupled waveguides with lossy center waveguide, Eq. (6). The decay rates Γ_k show the emergence of a slow mode near $\gamma_{PT} \sim 2\sqrt{2}J$ for a wide range of center-site potential. These results are even in δ and thus remain valid for $\delta < 0$.

$$\lambda_{t\pm} = -\frac{1}{2}(i\gamma + \delta + J') \pm \frac{1}{2}\sqrt{8J^2 + [(\delta - J') + i\gamma]^2}. \quad (9)$$

It follows from Eq. (9) that the exceptional point at $\delta = 0$ shown in Fig. 4 survives along the line $\delta = J'$. When $\delta \neq J'$, it is also straightforward to check that a slow mode emerges at a loss strength $\gamma_{\mathrm{PT}} \sim 2\sqrt{2}J$, even though the Hamiltonian H_t does not have an exceptional point.

It is worthwhile to mention that these trimer models cannot be identity-shifted to a PT-symmetric model that supports a purely real to complex-conjugate spectrum transition. That is, they are not isomorphic with any balanced gain-loss trimer models. They stand on their own and display the passive PT transition without an exceptional point over a wide range of Hamiltonian parameters. In the following section, we verify these results via BPM analysis of three planar coupled waveguides.

5. BPM ANALYSIS

The results presented in Section 4 are based on a tight-binding Hamiltonian where the spatial extent of a "site" is ignored. In a coupled-waveguides realizations of a lattice model, the electric field strength across the waveguide is not constant, and its spatial variation in the direction transverse to the waveguide needs to be taken into account. We verify our tight-binding results by obtaining the time evolution of the wave function $\psi(x,t)$ in a planar waveguide trimer with realistic parameters [42]. We remind the reader that $\psi(x,t)$ is the envelope of the actual electric field, i.e., $E(x,t) = \exp[ik_0 z - ic(k_0/n_0)t]\psi(x,t)$, where k_0 is the wavenumber of the rapidly varying part of the electric field, c is the speed of light, and n_0 is the real index of refraction of the cladding. Under paraxial approximation, the envelope $\psi(x,t)$ obeys the continuum Schrödinger equation for a particle with an effective mass $m = k_0 n_0^2/c$ in a potential $V(x) = ck_0[1 - n(x)^2/n_0^2]$. The position-dependent index of refraction $n(x)$ differs from that of a cladding only within each waveguide. For a small refractive-index contrast $\Delta n/n_0 \sim 10^{-4} \ll 1$, the potential becomes $V_p = 2ck_0\Delta n_p/n_0$ within waveguide p. We model the losses by adding negative imaginary parts to the index contrast Δn_p and generate different onsite potentials by choosing different real parts while satisfying the small-contrast constraint. (For more details regarding these calculations, see Refs. [42–44].)

Figures 6(a) and 6(b) show the resultant intensity plots $I(x,z) = |\psi(x, z = ct/n_0)|^2 dx$ for a dissipative trimer with an exceptional point, $\delta = 0$. The initial state is a symmetric combination of three single-waveguide eigenmodes with weight ratios 1:9:1. The symmetric combination ensures that the initial state is decoupled from the antisymmetric eigenmode with zero decay rate. Figure 6(a) shows the rapid decay of the initial pulse when the loss strength $\gamma/J = 2.75$ is just below the threshold $\gamma_{\mathrm{PT}} = 2\sqrt{2}J$. When the loss strength is increased fourfold to $\gamma/J = 10$, Fig. 6(b), the same pulse travels farther, signaling the emergence of the slowly decaying mode in the PT broken regime. Figures 6(c) and 6(d) show corresponding results for a trimer with no exceptional point and a very large onsite potential, $\delta/J = 1$. We use such a large offset because the BPM simulations are virtually indistinguishable from the $\delta = 0$ case for $\delta \lesssim J/2$. The eigenvalue flow in Fig. 4 shows that in this case, after an initial linear increase, the decay rate of the slow-mode Γ_2 does not change appreciably at large $\gamma \geq \gamma_{\mathrm{PT}}$. Figure 6(c) shows that when $\gamma/J = 2.75$, the initial pulse has a partial oscillation back into the central, lossy

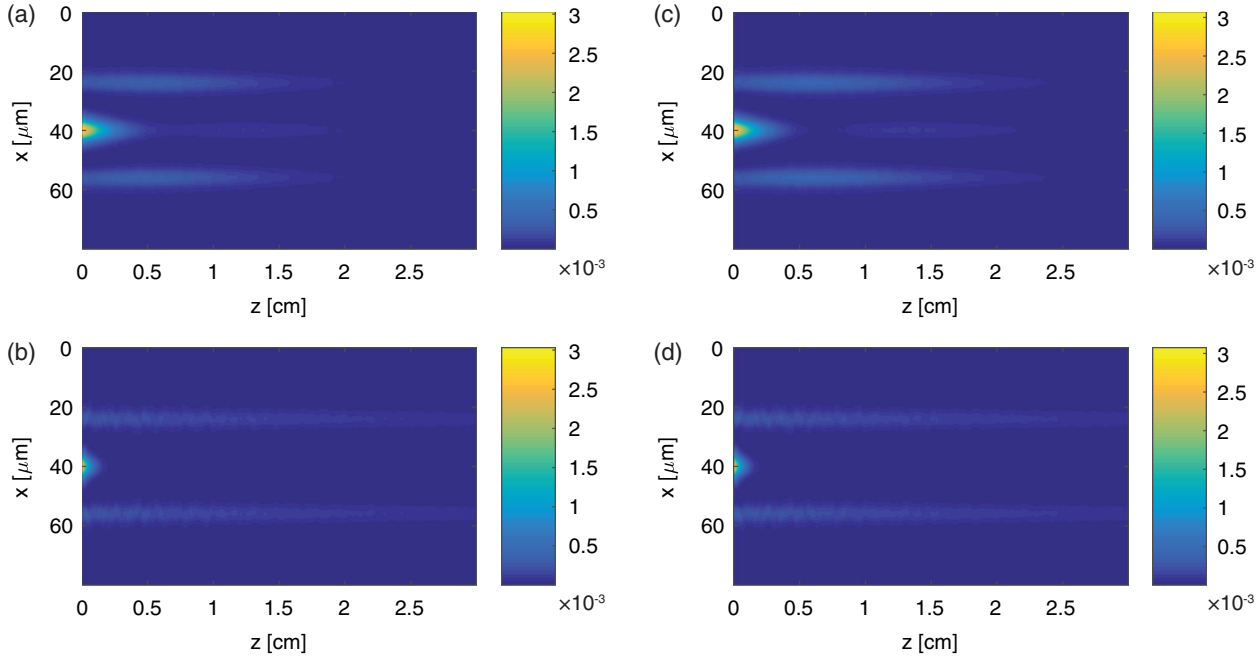

Fig. 6. BPM results for the intensity $I(x,z)$ of a symmetric initial pulse in a waveguide trimer defined by Hamiltonian Eq. (6) with (a), (b) $\delta = 0$ and (c), (d) $\delta/J = 1$. (a) When $\gamma/J = 2.75 < \gamma_{\mathrm{PT}}$, the pulse decays quickly. (b) At a much larger loss, $\gamma/J = 10$, the pulse propagates longer, giving rise to increased transmission. (c) For $\gamma/J = 2.75$, the pulse decays quickly. (d) At $\gamma/J = 10$, the pulse propagates longer. In both cases, $\delta = 0$ and $\delta/J = 1$, the emergence of a slowly decaying mode is clear; in the latter case, the Hamiltonian is far removed from an exceptional point.

waveguide. When the loss strength is increased to $\gamma/J = 10$, Fig. 6(d), the pulse travels farther, indicating a PT-broken regime. These representative BPM results are consistent with tight-binding model findings and show that, in dissipative systems, a PT transition can occur with or without exceptional points.

6. DISCUSSION

In this work, we have proposed a meaningful extension of the passive PT-symmetry-breaking phenomenon to dissipative Hamiltonians that are not identity-shifted from a balanced gain-loss Hamiltonian. We have shown that passive PT transitions, defined by the emergence of a slowly decaying mode, are ubiquitous in dissipative photonic systems and are not contingent on the existence of exceptional points. This is in sharp contrast with classical systems with balanced gain and loss, where PT-symmetry breaking and exceptional points go hand in hand, and the concept of PT-symmetry breaking cannot be meaningfully extended to unbalanced Hamiltonians. Our results may also be applicable to dissipative metamaterial systems, where nontrivial phenomena occur in the presence of balanced gain and loss [45,46].

Due to their exceptional tunability, relatively easy scalability, and the ability to implement one- and (postselected) two-qubit operations, integrated photonic systems at a quantum level are of great interest for quantum simulations and quantum computing. By introducing mode-dependent, tunable losses, such systems can be further tailored for true quantum simulations of non-Hermitian Hamiltonians in general and (dissipative) PT-symmetric Hamiltonians in particular. Such simulators will permit the investigation of quantum attributes, such as entropy, entanglement metrics, and many-particle correlations, across the passive PT transition. Carrying out such studies in balanced gain-loss systems remains an open question and, most likely, is fundamentally impossible [47].

Funding. National Science Foundation (NSF) (DMR 1054020).

REFERENCES

1. J. J. Sakurai, *Modern Quantum Mechanics* (Addison Wesley, 1996).
2. C. M. Bender and S. Boettcher, "Real spectra in non-Hermitian Hamiltonians having PT-symmetry," Phys. Rev. Lett. **80**, 5243–5246 (1998).
3. C. M. Bender, D. C. Brody, and H. F. Jones, "Complex extension of quantum mechanics," Phys. Rev. Lett. **89**, 270401 (2002).
4. C. M. Bender, D. C. Brody, and H. F. Jones, "Must a Hamiltonian be Hermitian?" Am. J. Phys. **71**, 1095–1102 (2003).
5. C. M. Bender, "Making sense of non-Hermitian Hamiltonians," Rep. Prog. Phys. **70**, 947–1018 (2007).
6. A. Mostafazadeh, "Pseudo-Hermiticity versus PT symmetry: the necessary condition for the reality of the spectrum of a non-Hermitian Hamiltonian," J. Math. Phys. **43**, 205–214 (2002).
7. A. Mostafazadeh, "Exact PT-symmetry is equivalent to Hermiticity," J. Phys. A **36**, 7081–7091 (2003).
8. A. Mostafazadeh and A. Batal, "Physical aspects of pseudo-Hermitian and PT-symmetric quantum mechanics," J. Phys. A **37**, 11645–11679 (2004).
9. A. Mostafazadeh, "Pseudo-Hermitian representation of quantum mechanics," Int. J. Geom. Methods Mod. Phys. **07**, 1191–1306 (2010).
10. M. Znojil, "Time-dependent version of crypto-Hermitian quantum theory," Phys. Rev. D **78**, 085003 (2008).
11. M. Znojil, "Three-Hilbert-space formulation of quantum mechanics," SIGMA **5**, 001 (2009).
12. R. El-Ganainy, K. G. Makris, D. N. Christodoulides, and Z. H. Musslimani, "Theory of coupled optical PT-symmetric structures," Opt. Lett. **32**, 2632–2634 (2007).
13. S. Klaiman, U. Gunther, and N. Moiseyev, "Visualization of branch points in PT-symmetric waveguides," Phys. Rev. Lett. **101**, 080402 (2008).
14. Y. N. Joglekar, C. Thompson, D. D. Scott, and G. Vemuri, "Optical waveguide arrays: quantum effects and PT symmetry breaking," Eur. Phys. J. Appl. Phys. **63**, 30001 (2013).
15. C. E. Rüter, K. G. Makris, R. El-Ganainy, D. N. Christodoulides, M. Segev, and D. Kip, "Observation of parity-time symmetry in optics," Nat. Phys. **6**, 192–195 (2010).
16. L. Feng, M. Ayache, J. Huang, Y.-L. Xu, M.-H. Lu, Y.-F. Chen, Y. Fainman, and A. Scherer, "Nonreciprocal light propagation in a silicon photonic circuit," Science **333**, 729–733 (2011).
17. A. Regensburger, C. Bersch, M.-A. Miri, G. Onishchukov, D. N. Christodoulides, and U. Peschel, "Parity-time synthetic photonic lattices," Nature **488**, 167–171 (2012).
18. B. Peng, S. K. Ozdemir, F. Lei, F. Monifi, M. Gianfreda, G. L. Long, S. Fan, F. Nori, C. M. Bender, and L. Yang, "Parity-time-symmetric whispering-gallery microcavities," Nat. Phys. **10**, 394–398 (2014).
19. M. Brandstetter, M. Liertzer, C. Deutsch, P. Klang, J. Schoberl, H. E. Tureci, G. Strasser, K. Unterrainer, and S. Rotter, "Reversing the pump dependence of a laser at an exceptional point," Nat. Commun. **5**, 4034 (2014).
20. B. Peng, S. K. Ozdemir, S. Rotter, H. Yilmaz, M. Liertzer, F. Monifi, C. M. Bender, F. Nori, and L. Yang, "Loss-induced suppression and revival of lasing," Science **346**, 328–332 (2014).
21. L. Feng, Z. J. Wong, R.-M. Ma, Y. Wang, and X. Zhang, "Single-mode laser by parity-time symmetry breaking," Science **346**, 972–975 (2014).
22. H. Hodaei, M.-A. Miri, M. Heinrich, D. N. Christodoulides, and M. Khajavikhan, "Parity-time-symmetric microring lasers," Science **346**, 975–978 (2014).
23. Z. Lin, H. Ramezani, T. Eichelkraut, T. Kottos, H. Cao, and D. N. Christodoulides, "Unidirectional invisibility induced by PT-symmetric periodic structures," Phys. Rev. Lett. **106**, 213901 (2011).
24. L. Feng, Y.-L. Xu, W. S. Fegadolli, M.-H. Lu, J. E. B. Oliveira, V. R. Almeida, Y.-F. Chen, and A. Scherer, "Experimental demonstration of a unidirectional reflectionless parity-time metamaterial at optical frequencies," Nat. Mater. **12**, 108–113 (2013).
25. G. S. Agarwal and K. Qu, "Spontaneous generation of photons in transmission of quantum fields in PT-symmetric optical systems," Phys. Rev. A **85**, 031802 (2012).
26. J. D. Huerta Morales and B. M. Rodriguez-Lara, "Photon propagation through linearly active dimers," Appl. Sci. **7**, 587 (2017).
27. R. El-Ganainy, K. G. Makris, M. Khajavikhan, Z. H. Musslimani, S. Rotter, and D. N. Christodoulides, "Non-Hermitian physics and PT symmetry," Nat. Phys. **14**, 11–19 (2018).
28. M. Ornigotti and A. Szameit, "Quasi PT-symmetry in passive photonic lattices," J. Opt. **16**, 065501 (2014).
29. A. Guo, G. J. Salamo, D. Duchesne, R. Morandotti, M. Volatier-Ravat, V. Aimez, G. A. Siviloglou, and D. N. Christodoulides, "Observation of PT-symmetry breaking in complex optical potentials," Phys. Rev. Lett. **103**, 093902 (2009).
30. L. Xiao, X. Zhan, Z. H. Bian, K. K. Wang, X. Zhang, X. P. Wang, J. Li, K. Mochizuki, D. Kim, N. Kawakami, W. Yi, H. Obuse, B. C. Sanders, and P. Xue, "Observation of topological edge states in parity-time-symmetric quantum walks," Nat. Phys. **13**, 1117–1123 (2017).
31. J. Li, A. K. Harter, J. Liu, L. de Melo, Y. N. Joglekar, and L. Luo, "Observation of parity-time symmetry breaking transitions in dissipative Floquet system of ultracold atoms," arXiv:1608.05061 (2016).
32. T. Kato, *Perturbation Theory for Linear Operators* (Springer, 1976).
33. H. Hodaei, A. U. Hassan, S. Wittek, H. Garcia-Garcia, R. El-Ganainy, D. N. Christodoulides, and M. Khajavikhan, "Enhanced

sensitivity at higher-order exceptional points," Nature **548**, 187–191 (2017).
34. W. Chen, S. K. Ozdemir, G. Zhao, J. Wiersig, and L. Yang, "Exceptional points enhance sensing in an optical microcavity," Nature **548**, 192–196 (2017).
35. W. D. Weiss and A. L. Sannino, "Avoided level crossing and exceptional points," J. Phys. A **23**, 1167–1178 (1990).
36. I. Rotter and A. F. Sadreev, "Avoided level crossings, diabolic points, and branch points in the complex plane in an open double quantum dot," Phys. Rev. E **71**, 036227 (2005).
37. H. Eleuch and I. Rotter, "Avoided level crossings in open quantum systems," Fortschr. Phys. **61**, 194–204 (2012).
38. M. Lietrzer, L. Ge, A. Cerjan, A. D. Stone, H. E. Tureci, and S. Rotter, "Pump-induced exceptional points in lasers," Phys. Rev. Lett. **108**, 173901 (2012).
39. R. El-Ganainy, M. Khajavikhan, and L. Ge, "Exceptional points and lasing self-termination in photonic molecules," Phys. Rev. A **90**, 013802 (2014).
40. M. H. Teimourpour and R. El-Ganainy, "Laser self-termination in trimer photonic molecules," J. Opt. **19**, 075801 (2017).
41. A. Szameit and S. Nolte, "Discrete optics in femtosecond-laser-written photonic structures," J. Phys. B: At. Mol. Opt. Phys. **43**, 163001 (2010).
42. J. M. Zeuner, M. C. Rechtsman, Y. Plotnik, Y. Lumer, S. Nolte, M. S. Rudner, M. Segev, and A. Szameit, "Observation of a topological transition in the bulk of a non-Hermitian system," Phys. Rev. Lett. **115**, 040402 (2015).
43. A. K. Harter, T. E. Lee, and Y. N. Joglekar, "PT-breaking threshold in spatially asymmetric Aubry-Andre-Harper models: hidden symmetry and topological states," Phys. Rev. A **93**, 062101 (2016).
44. A. K. Harter, F. A. Onanga, and Y. N. Joglekar, "Veiled symmetry of disordered Parity-Time lattices: protected PT-threshold and the fate of localization," Sci. Rep. **8**, 44 (2018).
45. Y. Fu, X. Zhang, Y. Xu, and H. Chen, "Design of zero index metamaterials with PT symmetry using epsilon-near-zero media with defects," J. App. Phys. **121**, 054503 (2017).
46. Y. Fu and Y. Xu, "Asymmetric effects in waveguide systems using PT symmetry and zero index metamaterials," Sci. Rep. **7**, 12476 (2017).
47. S. Scheel and A. Szameit, "PT-symmetric photonic quantum systems with gain and loss do not exist," arXiv:1805.10876 (2018).